ISSN 1063-7745, Crystallography Reports, 2012, Vol. 57, No. 5, pp. 751–757. © Pleiades Publishing, Inc., 2012
Original Russian Text © R.A. Khasanov, N.M. Nizamutdinov, N.M. Khasanova, V. M. Vinokurov, G.S. Morozov, A.O. Krivtsov, 2012, published in Kristallografiya, 2012, Vol. 57, No. 5, pp. 834–840.

On the 100th anniversary of the discovery of X-ray diffraction

Derivation of the Conditions for Equivalent Positions in Crystals: The Dissymmetrization of Barite by Electron Spin Resonance Spectra

R. A. Khasanov[a, b], N. M. Nizamutdinov[a], N. M. Khasanova[a], V. M. Vinokurov[†a], G. S. Morozov[a], and A. O. Krivtsov[c]

[a] *Kazan Federal University, Kazan, 420008 Russia*
e-mail: vladimir.vinokurov@ksu.ru
[b] *Central Research Institute for Geology of Industrial Minerals, Kazan, 420097 Russia*
[c] *Kazan State Technological University, Kazan, 420015 Russia*

Received August 29, 2011

Abstract—The conditions for equivalent positions on the (*hkl*) face of growing crystal are derived using symmetry elements of the space group. It is shown by the example of the sp. gr. D_{2h}^{16} that the conditions of equivalent position formation coincide with conditions of the reflection of diffracted beams by crystal. It is established that electron spin resonance (ESR) centers in barite, SO_4^- (I) and SO_4^- (II), with only two conjugate spectra with equal intensity out of four, and SO_4^- (III), with a different intensity of conjugate spectra $K_{\alpha M} = 2$, are localized into the growth pyramid of the (001) face with a [010] step. SO_2^-, SO_3^-,, and SO_4^-(IV) centers, having an identical intensity of the conjugate ESR spectra with $K_{\alpha M} = 2$, are localized into the growth pyramid of the (210) face with a growth step [001].

DOI: 10.1134/S1063774512050070

INTRODUCTION

The crystallization of a real crystal is a unified process of formation of a crystalline matrix and a system of its defects. This process occurs so that the result is a three-dimensional periodic structure. Under appropriate conditions, a growing face is parallel to the nodal net plane (*hkl*). The three-dimensional periodicity gives rise to 230 space groups G_C^q of crystal symmetry. These crystallization properties are independent of the chemical composition of crystal and are systematic. The dependence of structure on the chemical composition and growth conditions is reflected in the realization of one out of 230 groups of spatial symmetry. These geometric crystallographic positions lie in the basis of the diffraction methods for studying crystal structure [1], crystal growth theory [2–4], and an analysis of point defects and features of their distribution over subsystems of regular systems of points [5].

Electron spin resonance (ESR) revealed that dissymmetrization is due to the nonequivalent formation of positions on a growing face that are equivalent in the crystal structure. A theoretical-group analysis of dissymmetrization was developed in [5, 6] on the basis of point crystallographic groups G_C. When analyzing dissymmetrization at the level of point groups, it is assumed that the equivalent formation of equivalent structural positions occurs on a growth step oriented perpendicularly to the symmetry plane of the crystal point group. It is neglected that the symmetry plane can be a plane of grazing reflection and, as a consequence, the dependence of the structure dissymmetrization on the symbol (*hkl*) of the growing face is also disregarded.

Deriving the rules for the equivalent formation of positions during growth using elements of space group symmetry makes repeated analyses of specific structures unnecessary and allows one to tabulate results for each space group.

The purpose of this study was to analyze crystal growth using symmetry elements of the structure space group. The following stages of the investigation are selected: analysis of the equivalent formation of systems of translationally equivalent points of one regular system of points during crystal growth, a study of dissymmetrization in barite ($BaSO_4$) single crystals (based on the ESR spectra of intrinsic paramagnetic centers), and a comparison of the results of an analysis of the growth processes and the experimental study of barite. Barite was chosen as an object of study because its growth features have been reliably established [7].

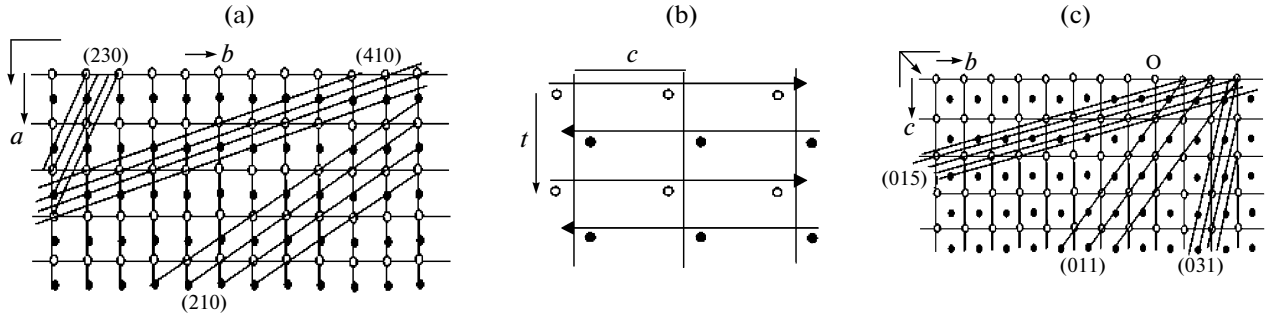

Fig. 1. Points that are symmetrically equivalent with respect to planes of types (a) **a**: location in the (*hk*0) planes, $h = 2n$, n is an arbitrary integer, and (c) **n**: location in the (0*kl*) planes, $k + l = 2n$; panel (b) shows a periodical change in the kink motion direction when a step passes from one equivalent position to another.

EQUIVALENT FORMATION OF A SYSTEM OF TRANSLATIONALLY EQUIVALENT POINTS OF ONE REGULAR SYSTEM OF POINTS DURING CRYSTAL GROWTH

There are two main mechanisms of crystal growth: normal and layer-by-layer [3, 8].

(i) Under normal growth conditions, particle adhesion to atomic-rough surfaces occurs at any site; from the macroscopic point of view [8], the surface shifts along the normal to itself at each point during growth. The distribution of point defects over a system of translationally equivalent points (STEP) in a system of regular points correspond to face symmetry group; this circumstance allows one to investigate the formation of equivalent positions using a point symmetry group.

(ii) In the case of layer-by-layer growth, it is necessary to separately investigate the formation of systems of translationally equivalent positions relative to the symmetry planes and axes of the structure.

One important element of the growing-crystal face is a kink. The attachment of a new particle to a kink does not change the number of uncompensated bonds or the surface energy; i.e., the initial surface configuration is reproduced (see p. 21 in [8]). The work done to transfer a particle from some other positions on the surface to the growth medium is not equal to the chemical potential difference, since the surface energy changes in this case. Therefore, the attachment of new particles to a kink means crystal growth.

The propagation of a growth step due to the deposition of material should be a periodical process, reflecting a sequence of equivalent positions of the step structure and kink, as well as the growing-face structure. There are two forms of equivalence for the layer configuration during the deposition of material: translational and orientational.

In this paper we report the results of studying the orientational equivalence of the growing surface configuration. The orientational equivalence of a growing surface is determined by the symmetry elements of the (*hkl*) face onto which material is deposited. The elements of face symmetry are the elements of structure symmetry that are oriented perpendicularly to faces. Such are symmetry planes and axes.

Crystal growth is in essence the formation of crystal structure and its symmetry elements. The formation of structures with screw axes and planes of grazing reflection (symmetry elements with conjugate parallel translations $\boldsymbol{\sigma} \neq \mathbf{t}$, where $\mathbf{t}$ is a lattice vector) significantly differs from the formation of structures with symmetry axes and planes without conjugate vectors $\boldsymbol{\sigma}$ [2], and the formation of screw axes differs from the formation of grazing reflection planes.

The only symmetry element that allows for the transformation of the step and face of a growing layer into the equivalent position is the structure symmetry plane if it is oriented perpendicularly to the face and its growth step.

We assume that the growth layer height is equal to the interplanar spacing d_{hkl}. Let us consider the equivalent formation of positions on the growth layer step with respect to the symmetry plane of the layer structure by the example of the sp. gr. $Pnma - D_{2h}^{16}$ of barite. There are three types of symmetry planes in the structure: **n**, **m**, and **a**. Let us consider each type of planes separately.

*Grazing-reflection plane of the **a** type.* In the *Pnma* system, the symmetry operation with respect to the **a** plane has the form $\mathbf{a} = (\mathbf{m}_z, \mathbf{a}/2)$; it includes $\mathbf{m}_z$ (reflection with respect to the plane oriented perpendicularly to the **z** crystallographic axis) and $\mathbf{a}/2$ (subsequent parallel translation after the reflection, i.e., conjugate with $\mathbf{m}_z$). Infinite STEP ($STEP_1$), which is geometrically represented by a space lattice, is formed when an arbitrary point (Fig. 1a, white circle) of crystal space is multiplied by parallel translations of group *P*. The reflection of $STEP_1$ with respect to the **a** plane generates $STEP_2$ (Fig. 1a, shaded circles).

We will determine the condition of equivalent formation of $STEP_1$ and $STEP_2$ points on a growing face. Let the growing face be parallel to a plane belonging to the (*hkl*)-type nodal net, i.e., be perpendicular to the

reciprocal lattice vector $\mathbf{H}_{hkl} = h \cdot \mathbf{a}^* + k \cdot \mathbf{b}^* + l \cdot \mathbf{c}^*$. According to the principle of reconstruction of equivalent spatial configurations of the crystal surface during growth, the growing face should be perpendicular to a symmetry plane of type **a**; i.e., $\mathbf{H}_{hkl} \perp \mathbf{c}$ or the scalar product $(\mathbf{H}_{hkl} \cdot \mathbf{c})$ of the vectors $\mathbf{H}_{hkl}$ and **c** must be zero: $(\mathbf{H}_{hkl} \cdot \mathbf{c}) = 0$. Since $(\mathbf{H}_{hkl} \cdot \mathbf{c}) = l$, $l = 0$. Thus, $l = 0$ is the condition of mutual perpendicularity of the growing face and symmetry plane.

The (hk0) planes of nodal nets divide the periods **a** and **b** into h and k equal parts, respectively, i.e., into segments equal to $\mathbf{a}/h$ and $\mathbf{b}/k$. If $h = 2n$ (n is an integer), the lengths of segments along the **a** axis are $\mathbf{a}/(2n) = (\mathbf{a}/2)/n$, i.e., planes of nodal nets divide both **a** and $\mathbf{a}/2$ into equal parts. This means that the planes of the (hk0) type contain both $STEP_1$ and $STEP_2$ at $h = 2n$.

The period **t** of the (hk0) face, oriented perpendicularly to the [001] axis, is $\mathbf{t} = V/(\mathbf{c} \cdot d_{hk0})$, where V is the Bravais cell volume and d_{hk0} is the interplanar spacing (Fig. 1b). The kink motion should change with a step $\mathbf{t}/2$ of the step propagation. For barite, such faces are x (230), m (210), λ (410), and b (010) (Fig. 1b).

Thus, one can conclude that, when material is deposited during growth on an (hk0)-type face ($h = 2n$), positions are formed pairwise equivalent to the **a** plane if the growth step is perpendicular to this plane. This is also valid at $h = 0$.

*Plane of the **n** type.* The symmetry operation with respect to the **n** plane has the form $\mathbf{n} = (\mathbf{m}_x, (\mathbf{b} + \mathbf{c})/2)$, where $\mathbf{m}_x$ is a reflection of a point with respect to the (100) plane and $(\mathbf{b} + \mathbf{c})/2$ is a subsequent parallel translation, conjugate with $\mathbf{m}_x$. The planes of nodal nets oriented perpendicularly to the **n** plane have the indices (0kl). If the point O is multiplied in space using a group of parallel translations, we obtain $STEP_1$ (Fig. 1c, white points). The action of a plane of the $\mathbf{n} = (\mathbf{m}_x, (\mathbf{b} + \mathbf{c})/2)$ type on $STEP_1$ generates $STEP_2$ (Fig. 1c, shaded points). $STEP_1$ and $STEP_2$ are orientationally equivalent systems, which are geometrically represented by the corresponding equivalent space lattices, shifted after the $\mathbf{m}_x$ reflection by the vector $(\mathbf{b} + \mathbf{c})/2$ with respect to each other.

Each equivalent space lattice can be presented as a system of parallel planes of nodal nets (0kl) (Fig. 1c). To make sites of these two lattices lie in the same plane, the systems of planes of nodal nets (0kl) corresponding to $STEP_1$ and $STEP_2$ must coincide. This occurs when planes divide the vector $(\mathbf{b} + \mathbf{c})/2$ into n equal parts.

The equation of a net plane with indices (0kl), closest to the origin of coordinates, has the form $k \cdot \mathbf{y}/\mathbf{b} + l \cdot \mathbf{z}/\mathbf{c} = 1$. For the plane with the number n, containing a point specified by the vector $(\mathbf{b} + \mathbf{c})/2$, this equation will take the form $k \cdot \mathbf{y}/\mathbf{b} + l \cdot \mathbf{z}/\mathbf{c} = n$. Using the coordinates $\mathbf{y} = \mathbf{b}/2$ and $\mathbf{z} = \mathbf{c}/2$ of the point, the latter equation can be written in the form of equality $(k + l)/2 = n$ or $(k + l) = 2n$. Such are the o (011) faces; more rare ones are Ω (031) and j (035).

Thus, we can conclude that the points equivalent with respect to a plane of the $\mathbf{n} = (\mathbf{m}_x, (\mathbf{b} + \mathbf{c})/2)$ type are formed pairwise and equivalently during the deposition of material on the faces (0kl) under the condition $(k + l) = 2n$; the growth step is directed along [100].

The plane of the $\boldsymbol{m} = (\boldsymbol{m}_y, 0)$ type includes the reflection $\mathbf{m}_y$ with respect to the (010) plane. The vector conjugate with the $\mathbf{m}_y$ plane is zero in modulus (mod P). The points that are equivalent with respect to the **m** plane are formed equivalently during the deposition of material if the growing face (h0l) and its growth step are perpendicular to the **m**-type plane; limitations are not imposed on the indices h and l. Such are the a (100), w (103), l (102), d (101), and u (201) faces.

GROWTH FEATURES OF ORIENTATIONALLY EQUIVALENT LAYERS OF SYMMETRY AXES

Let us consider a system of points that are equivalent with respect to the screw axis $2_{1z} = (2_z, \mathbf{c}/2)$. The symmetry operation includes rotation 2_z and conjugate parallel translation $\mathbf{c}/2$. $STEP_1$ and $STEP_2$ are transformed into each other (Fig. 2). It is known that layers 1 and 2 of thickness $\mathbf{c}/2$ can grow separately [7]. In barite, these layers propagate successively in the opposite directions (Fig. 2)

Equivalent positions are located in neighboring layers of thickness $\mathbf{c}/2$. They are equivalently formed under the condition that each surface layer $\mathbf{c}/2 = d_{001}/2$ grows separately, being imposed on the previous layer and having an opposite propagation direction

The equivalence of points with respect to 2_{1z} is violated when the growing-layer height is equal to an integer number of interplanar spacings d_{001}. The growing layer includes a system of layers with thickness $d_{001}/2$ that grow "well" and "poorly" in this direction. The system of layers with preferred propagation direction forms conditions for the growth of a system of layers that grow poorly in this direction [8].

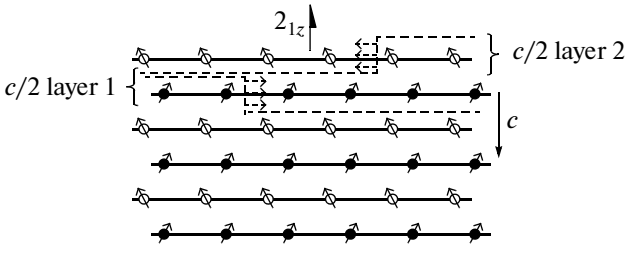

Fig. 2. System of points equivalent with respect to the screw axis 2_{1z}; $STEP_1$ and $STEP_2$ (white and black circles, respectively) belong to equivalent layers of thickness $\mathbf{c}/2$.

It was experimentally established for barite [7] that the layers equivalent with respect to the screw axis 2_{1z}, having their preferred growth directions, may be generalized for any screw axis n_s, where n is an order of the symmetry axis, s is an integer, and $1 \le s \le n$. If **t** is the shortest lattice vector along the symmetry axis of order n, the vector $\boldsymbol{\sigma}_{ns}$, conjugate with the n_s axis, is $\boldsymbol{\sigma}_{ns} = (s/n) \cdot \mathbf{t}$. The number and thickness of layers equivalent with respect to the n_s axis are $n' = n/D$ and $\mathbf{t}/n'$, where D is the largest general divider of the numbers n and s. We assume that the upper layer is the layer of thickness $\mathbf{t}/n'$, the preferred growth of which is facilitated by this growth-step propagation direction. If the growth step has some other equivalent propagation direction, the upper layer will be that which is facilitated by this equivalent growth step. Each equivalent step propagation direction corresponds to a layer of thickness $\mathbf{t}/n'$ equivalent with respect to the screw axis n_s. Equivalent layers of thickness $\mathbf{t}/n'$ and the corresponding favorable equivalent step propagation directions are determined by the same screw axis n_s. The interfaces of these regions of material deposition can be found from the rearrangement of the intensities of conjugate ESR spectra of the samples selected from these equivalent growth regions.

In the case of sp. gr. $Pnma - D_{2h}^{16}$, the central symmetry of ESR spectra does not make it possible to differentially record spectra of paramagnetic centers of both layers with a thickness $\mathbf{c}/2$ linked by the screw axis 2_{1z}. These layers are transformed into each other via the inversion center of the barite structure under consideration. The layer with thickness $\mathbf{c}/2$ includes structural units (equivalent with respect to the 2_{1x} axis) of the **a**- and **m**-type planes. When a growth pyramid of the (001) face is formed during the deposition of material on steps oriented perpendicularly to the symmetry planes **m**, systems of translationally equivalent points (equivalent with respect to the **a**-type plane) are formed nonequivalently. This nonequivalence causes dissymmetrization in the layer with thickness $\mathbf{c}/2$; it should be reflected in the ESR spectra of centers with the magnetic multiplicities $K_{\alpha M} = 2$ and $K_{\alpha M} = 4$.

ESR IN BARITE SINGLE CRYSTAL

ESR spectra of barite single crystals were investigated in [9]. The presence of the following paramagnetic centers was established: SO_2^-, SO_3^- (I), SO_3^- (II), SO_4^-, SO_4^- (I) + Y^{3+}, SO_4^- (II) + Y^{3+}, SO_4^{3-}, O^- (I), O^- (II), O^- (III), and SO_3^+. The latter three centers were studied at 77 and the others were analyzed at 300 K. All centers, except SO_3^+, exhibit ESR spectra with a multiplicity $K_{\alpha M} = 2$, i.e., occupy positions of type 4(c) with the symmetry group $G_\alpha = C_S$. The ESR spectrum of the SO_3^+ center has a multiplicity $K_{\alpha M} = 4$, which corresponds to the position of 8(d) type with $G_\alpha = C_1$.

In this study the ESR spectra of a barite single crystal were studied on a PS-100X spectrometer (Belarussian State University, Minsk) with the resonant frequency $\nu = 9.139$ GHz at room temperature. This instrument, unlike that used in [9], has a higher sensitivity and is equipped with a Hall probe.

The crystal shape is specified by the {210} prism and {001} pinacoid. The crystal orientation in a magnetic field was set and corrected according to the superposition schemes of ESR spectra [10], which are determined by the position group G_α of the paramagnetic center and the point symmetry group G_C of the crystal; sp. gr. $Pnma - D_{2h}^{16}$ allows four types of positions: $8d - G_\alpha = C_1$, $4c - G_\alpha = C_S$, $4b - G_\alpha = C_i$, and $4a - C_i$ [1], which are characterized, respectively, by the magnetic multiplicities $K_{\alpha M}(d) = 4$, $K_{\alpha M}(c) = 2$, $K_{\alpha M}(b) = 4$, and $K_{\alpha M}(a) = 4$. The structural Ba^{2+}, S^{6+}, O_I^{2-}, and O_{II}^{2-} ions occupy positions of the 4c type, corresponding to the ESR spectra with $K_{\alpha M}(c) = 2$, while the O_{III}^{2-} and O_{IV}^{2-} ions occupy the 8d positions, which correspond to the spectra with $K_{\alpha M}(d) = 4$.

The ESR spectra of the barite sample under study had $K_{\alpha M} = 2$ and $K_{\alpha M} = 4$. The magnetic multiplicity $K_{\alpha M} = 2$ corresponds to one type of positions, 4c, while the multiplicity $K_{\alpha M} = 4$ corresponds to three types of positions: 8d, 4b, and 4a. The ESR spectrum with $K_{\alpha M} = 2$ should have an isolated axis parallel to [010], while the other two transition axes must lie in the (010) plane. For the spectrum with $K_{\alpha M} = 4$, the transition axes have a skew orientation with respect to the crystal symmetry elements.

The conjugate spectra with $K_{\alpha M} = 2$ at $\mathbf{H} \parallel (100)$ and (001) merge pairwise but are observed separately at $\mathbf{H} \parallel (010)$. The conjugate spectra with $K_{\alpha M} = 4$ merge pairwise into one spectrum when the external-field vector **H** is parallel to any of three planes: (100), (010), or (001)

The angular dependences of the ESR spectra at $\mathbf{H} \parallel (100)$, (010), and (001) were studied to determine the parameters of the spin Hamiltonian (SH) of paramagnetic centers and the type of crystal dissymmetrization (Fig. 3).

The barite crystal under study differs from that described in [9] by the existence of two additional spectra with $K_{\alpha M} = 4$ from the SO_4^- (I) and SO_4^- (II) centers and one spectrum with $K_{\alpha M} = 2$ from the SO_4^- (IV) centers (Fig. 3). The spectra are described by the SH in the form [11]

$$\mathbf{H} = \beta \hat{S} g \mathbf{H}, \quad S = 1/2, \quad g_{ij} = g_{ji}. \qquad (1)$$

The spectrum of SO_4^- (IV) with $K_{\alpha M} = 2$ is characterized by the following principal values of the g ten-

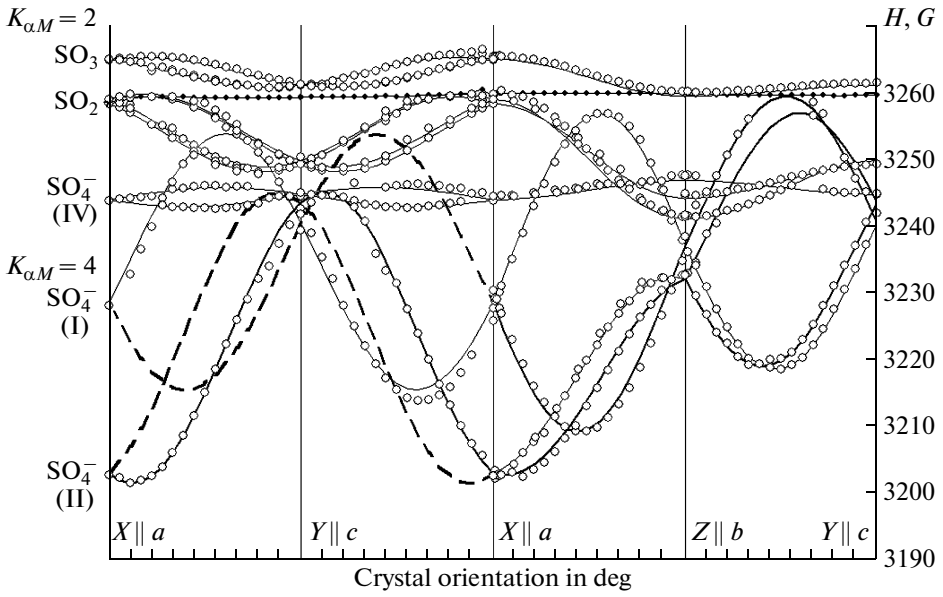

Fig. 3. Angular dependences of the (circles) and experimental (line) calculated values **H** of the magnetic field for the ESR spectral lines in three orthogonal planes of barite crystal. The dotted lines select disymmetrized centers in the (010) plane.

sor: 2.0107, 2.0124, and 2.0097 (Fig. 3). The principal axis with the value of 2.0097 is parallel to the [010] axis, while the principal axis with 2.0124 makes an angle of 47.7° with the [001] axis. This hole center is characterized by a low anisotropy of the *g* tensor. Centers of this type were observed previously [9] in anhydrite and celestine single crystals. The PO_4^{2-} center in anhydrite was interpreted more reliably. Its spectrum is characterized by an isotropic hyperfine structure ($A_{iso} = 28.5$ G), which is responsible for the interaction with the nuclear spin $I = 1/2$, and the following principal values of the *g* tensor: 2.0160, 2.0126, and 2.0095. By analogy with PO_4^{2-}, this center in barite can be attributed to the isoelectronic hole center SO_4^- (IV) in the regions of the isovalent substitution of Ba^{2+} ions with such impurity ions as Ca^{2+} and Sr^{2+}.

DISCUSSION AND CONCLUSIONS

The paramagnetic centers SO_2^-, SO_3^-,and SO_4^- (IV) in the crystal under study have a magnetic multiplicity $K_{\alpha M} = 2$, and their conjugate spectra have equal intensities. The equality of intensities suggests that they are located in the growth pyramid of (*hk*0)-type faces with $h = 2n$. In the barite crystal under consideration, the developed faces of the {210} orthorhombic prism belong to this type.

The paramagnetic centers SO_4^- (I) and SO_4^- (II) have a magnetic multiplicity $K_{\alpha M} = 4$; according to the principal values of the *g* tensor, they correspond to tetrahedral complexes and occupy general-type positions 8*d* in the structure. The SO_4^- (I) and SO_4^- (II) centers are SO_4^{2-} tetrahedra with a deficit of one electron in the domain of formation of *V*1 and *V*2 vacancies of Ba^{2+} ions (Fig. 4). The decrease in the symmetry of the tetrahedral position from C_s to C_1 is caused by the fact that Ba^{2+} vacancies and the corresponding centers are located in adjacent symmetry planes of the structure. With respect to the SO_4^{2-} tetrahedron, there are two Ba^{2+} ions in the adjacent symmetry plane: one at dis-

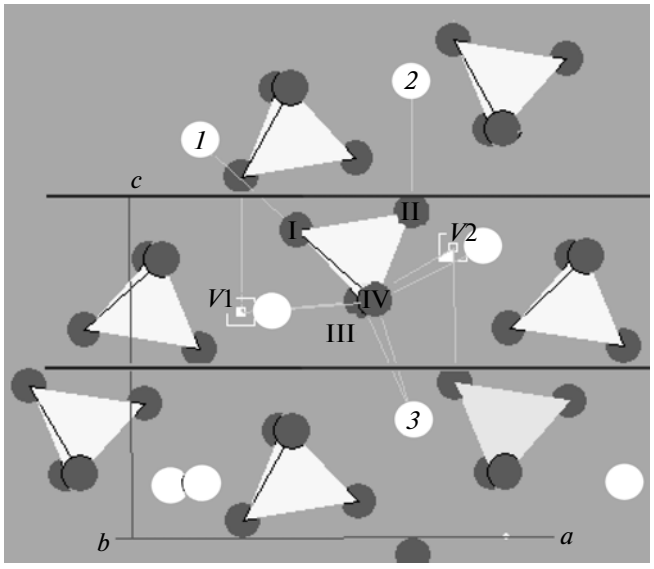

Fig. 4. Projection of barite structure on the (010) plane, where *V*1, *V*2 are Ba^{2+} ion vacancies; [SiO_4] tetrahedra with vertices (I, II, III, IV) and Ba^{2+} ions (*1*, *2*, and *3*) are selected. Lines of cleavage planes are drawn.

Parameters of the *g* tensor of the SH of centers in positions with the groups $G_\alpha = C_S(SO_3^-, SO_2^-)$ and $C_1(SO_4^-$ (I), SO_4^-(II))

Axes	Orientation of the *g*-tensor principal axes			Axes	Orientation of the *g*-tensor principal axes		
SO_3^-	**a**	**c**	**b**	SO_2^-	**a**	**c**	**b**
1.9999	15.42°	74.57°	90°	2.0036	18.10°	71.89°	90°
2.0026	105.43°	15.42°	90°	2.0104	108.11°	18.10°	90°
2.0034	90°	90°	0.0°	2.0129	90°	90°	0.0°
SO_4^- (I)	**a**	**c**	**b**	SO_4^- (II)	**a**	**c**	**b**
2.0387	11.39°	78.64°	88.93°	2.0434	49.77°	119.95°	125.29°
2.0033	98.64°	36.60°	125.24°	2.0065	43.34°	50.76°	74.55°
2.0275	97.38°	55.75°	35.26°	2.0021	76.56°	126.31°	39.51°

tances of 2.81 and 3.32 Å from the tetrahedron vertices (III, I) and the other at distances of 3.07 and 2.82Å from the tetrahedron vertices (II, III) (Fig. 4). In accordance with the vacancies of these ions, two ESR spectra of SO_4^- (I) and SO_4^- (II) centers are observed. The principal axis with $g = 2.0275$ of the SO_4^- (I) center makes angles of 97.38°, 35.26°, and 55.75° with the **a**, **b**, and **c** axes, respectively (table). Its direction practically coincides with that of the $S-O_{III}$ bond, which has direction angles of 95.80°, 36.07°, and 54.55° and is tilted with respect to the symmetry plane of the structural tetrahedron. In this case, SO_4^- (I) is represented by the vacancy *V*1 of the Ba^{2+} ion (Fig. 4).

The principal axis with $g = 2.0065$ of the SO_4^- (II) center, which makes angles of 43.34°, 74.55°, and 50.76° with the **a**, **b**, and **c** axes, respectively (table), is close to the $S-O_{II}$ bond (direction angles 43.32°, 90°, and 46.68°) of the structural tetrahedron. In this case, the charge compensator for the SO_4^- (II) center is represented by the vacancy *V*2 of the Ba^{2+} ion (Fig. 4). The deviation of the principal axis of the *g* tensor from the symmetry plane by an angle of 15.45° is caused by the repulsion of oxygen ions in the vicinity of the Ba^{2+} vacancy.

In the ESR spectra of SO_4^- (I) and SO_4^- (II), dissymmetrization is accompanied by a lowering of the tetrahedral position symmetry. In this case, Ba^{2+} vacancies and paramagnetic centers of the SO_4^- type are located in one layer of thickness **c**/2. The presence of dissymmetrization indicates the absence of translational diffusion of both barium ions and sulfate groups in this layer.

Previously, dissymmetrization in barites was also observed in the ESR spectra of the hole center O^- (III) with $K_{\alpha M} = 2$, i.e., when the Ba^{2+} vacancy does not lower the symmetry of the tetrahedral position [9]. One specific feature of this center is that its magneto-conjugate spectra differ in intensity. The intensity ratio of the magneto-conjugate spectra changes from sample to sample in the range of (1 : 1)–(1 : 10). The O^- (III) center is characterized by the principal values of the *g* tensor $g_{xx} = 2.0685$, $g_{yy} = 2.0086$, and $g_{zz} = 1.9997$ and the anisotropic superfine structure due to the ^{135}Ba and ^{137}Ba isotope.

This center can be presented as a paramagnetic tetrahedron SO_4^- (III) in the vicinity of the Ba^{2+} vacancy. The principal axis with $g_{zz} = 1.9997$ makes an angle of 47° with the [001] direction in the crystal and almost coincides with the $S-O_{II}$ bond in the tetrahedron, which makes an angle of 46.69° with the [001] direction. All three Ba^{2+} ions (*1*, *2*, and *3* in Fig. 4) around the SO_4^- tetrahedron, which are located in its local symmetry plane, belong to adjacent equivalent layers with a thickness **c**/2. Accordingly, the paramagnetic center SO_4^- (III) and the compensating vacancy Ba^{2+} are located in adjacent equivalent layers of height **c**/2 and are formed in the growth pyramids of the (001) face during the deposition of material on the steps oriented perpendicularly to the symmetry plane **m**. The disymmetrized distribution of defects with $K_{\alpha M} = 2$ over the system of translationally equivalent points suggests the absence of translational diffusion of barium ions and SO_4^- groups between layers of thickness **c**/2, which causes the uniform distribution of point defects in a regular system of points.

Note that the conditions of the equivalent formation of positions on the (*hkl*) face of the growing crystal coincide with those for the reflection of diffracted beams caused by the symmetry elements of the crystal structure [1, 12]. The introduction of symmetry elements of space groups makes it possible to specify the distribution regularities for impurity ions and point defects, which are caused by growth processes, as well as the dynamics processes in crystal structural units.

REFERENCES

1. *International Tables for Crystallography. Brief Teaching Edition of V. A SPACE-GROUP SYMMETRY*, Ed. by

T. Hahn (D. Reidel Publishing Company, Dordrecht, 1988).

2. J. D. H. Donnay and D. Harker, Am. Mineral. **22** (5), 446 (1937).
3. W. K. Burton, N. Cabrera, and F. C. Frank, Philos. Trans. R. Soc. London A Mathem. Phys. Sci. **243** (866), 299 (1951).
4. P. Hartman and W. G. Perdok, Acta Crystallogr. **8**, 49 (1955).
5. N. M. Nizamutdinov, G. R. Bulka, N. M. Khasanova, et al., Sov. Phys. Crystallogr. **22** (4), 445 (1977).
6. G. R. Bulka, V. M. Vinokurov, N. M. Nizamutdinov, and N. M. Hasanova, Phys. Chem. Miner. **6**, 283 (1980).
7. C. M. Pina, D. Bosbach, M. Prieto, and A. Putnis, J. Cryst. Growth **187** (1), 119 (1998).
8. A. A. Chernov, E. I. Givargizov, Kh. S. Bagdasarov, et al., *Modern Crystallography*, Vol. 3: *Crystal Growth*, *Modern Crystallography*, (Nauka, Moscow, 1980) [in Russian].
9. R. A. Khasanov, Candidate's Dissertation in Physics and Mathematics (Kazan, 1980).
10. N. M. Nizamutdinov, Doctoral Dissertation in Physics and Mathematics (Kazan, 2000).
11. S. A. Al'tshuler and B. M. Kozyrev, *Electron Spin Resonance in Compounds of Intermediate-Group Elements* (Nauka, Moscow, 1972) [in Russian].
12. G. B. Bokii and M. A. Poraí-Koshits, *X-Ray Structure Analysis* (Mosk. Gos. Univ., Moscow, 1964) [in Russian].

Translated by A. Grudtsov